Taylor & Francis
Taylor & Francis Group

Microvascular Rheology and Hemodynamics

HERBERT H. LIPOWSKY

Department of Bioengineering, The Pennsylvania State University, University Park,
Pennsylvania, USA

ABSTRACT

The goal of elucidating the biophysical and physiological basis of pressure–flow relations in the microcirculation has been a recurring theme since the first observations of capillary blood flow in living tissues. At the birth of the Microcirculatory Society, seminal observations on the heterogeneous distribution of blood cells in the microvasculature and the rheological properties of blood in small bore tubes raised many questions on the viscous properties of blood flow in the microcirculation that captured the attention of the Society's membership. It is now recognized that blood viscosity in small bore tubes may fall dramatically as shear rates are increased, and increase dramatically with elevations in hematocrit. These relationships are strongly affected by blood cell deformability and concentration, red cell aggregation, and white cell interactions with the red cells and endothelium. Increasing strength of red cell aggregation may result in sequestration of clumps of red cells with either reductions or increases in microvascular hematocrit dependent upon network topography. During red cell aggregation, resistance to flow may thus decrease with hematocrit reduction or increase due to redistribution of red cells. Blood cell adhesion to the microvessel wall may initiate flow reductions, as, for example, in the case of red cell adhesion to the endothelium in sickle cell disease, or leukocyte adhesion in inflammation. The endothelial glycocalyx has been shown to result from a balance of the biosynthesis of new glycans, and the enzymatic or shear-dependent alterations in its composition. Flow-dependent reductions in the endothelial surface layer may thus affect the resistance to flow and/or the adhesion of red cells and/or leukocytes to the endothelium. Thus, future studies aimed at the molecular rheology of the endothelial surface layer may provide new insights into determinants of the resistance to flow. *Microcirculation* (2005) **12,** 5–15. doi:10.1080/10739680590894966

KEY WORDS: blood viscosity, flow, intravascular pressure, rheology, shear rates, wall shear stress

INTRODUCTION

At the birth of the Microcirculatory Society in 1954, relatively little was known of the rheological behavior of blood in the microcirculation. The seminal studies of Poiseuille (54), Landis (39), Fåhraeus (20), Vejlens (68), and Krogh (38) provided a conceptual framework for understanding the basis for the resistance to flow. Although best known for his experimental studies of the flow of fluids through tubes, Poiseuille's earlier observations on the separation of cells and plasma in arterioles and venules led to the discovery of "plasma skimming" and the need for a greater understanding of the mechanics of blood flow (67). The pioneering intravital studies of Landis,

using a forerunner of the modern servo-null technique to measure capillary pressure, attempted to explore the applicability of Poiseuille's law to describe microvascular resistance. Fåhraeus' discovery of reductions in tube hematocrit as blood flows through small bore tubes, and subsequent studies on the attendant reduction in blood viscosity (21), defined the approach to elucidating the rheological basis of microvascular blood flow. The comprehensive experimental studies on leukocyte behavior in the microvasculature by Vejlens delineated many features of their distribution and sequestration in the microcirculation that affect blood flow. The pioneering observations by Krogh delineated many facets of flow distribution through networks of capillaries and sequestration of red cells under normal and pathological conditions.

However, it would take the subsequent five decades to develop a comprehensive understanding of the role for the intrinsic properties of blood and microvascular topography as determinants of the resistance to flow. Due to the advent of new quantitative methods for intravital microscopy, it is now well understood that in addition to blood cell concentration, red cell

deformability and aggregation and white blood cell deformability and adhesion to the endothelium are the principal intrinsic factors that affect resistance to flow. The extent to which they affect resistance is determined by topographical branching patterns and microvessel diameters. During the last five decades, numerous contributions by members of the Microcirculatory Society have explored the details of these interactions in health and disease. A brief overview of some of these studies that have set the stage for future studies of interactions between blood rheology and microvascular function is presented in the following.

THE *IN VITRO* FRAMEWORK

Acquisition of the viscosity of blood by bulk viscometry has emphasized the importance of shear rate, hematocrit, and red cell aggregation and deformability as it pertains to flow in large blood vessels (11). With the use of tube, Couette, and cone-plate viscometers, under the assumption that blood is a homogeneous fluid with an intrinsic viscosity, *in vitro* studies have revealed that blood viscosity falls about 75% as shear rates ($\dot{\gamma}$) rise from on the order of 0.1 to 1000 sec^{-1}. A comparison of this "shear thinning" of blood in the presence and absence of aggregating agents suggests that about 75% of the decrease is a result of the disruption of red cell aggregates, and 25% is due to red cell deformation in response to increased shear stresses. At a given shear rate, blood viscosity rises exponentially with increasing red blood cell (RBC) concentration (hematocrit) to a degree dependent on prevailing $\dot{\gamma}$. The viscosity of the suspending medium (plasma) has been shown to be invariant with $\dot{\gamma}$ (Newtonian) and is dependent mainly on protein content and temperature.

Within the circulation, in large diameter vessels representative of the macrocirculation (i.e., >100 μm), blood may be treated as a homogeneous continuum with intrinsic properties characterized by an "apparent viscosity." The term apparent viscosity is used since viscosity of a homogeneous fluid (e.g., water, molasses) is a material property that may be dependent on shear rate and temperature and is invariant with the size of the vessel through which it flows. *In vivo*, ever diminishing length scales and the particulate nature of blood affect this relationship as blood courses its way through successive divisions of the circulatory tree. The term "effective viscosity" (η) is often used to represent the value of viscosity that satisfies Poiseuille's law, since it does not explicitly

reflect the shear dependency of viscosity along the tube radius.

According to Poiseuille's law, flow (Q) and pressure drop (ΔP) are related by

$$Q = \frac{\pi}{128} \frac{D^4}{\eta l} \Delta P \qquad (1)$$

where D is luminal diameter and l is vessel length. Hence, given measurements of Q and ΔP, one may calculate η for a microvessel of specified length and diameter. The dominance of noncontinuum effects in the smallest microvessels (approaching red cell diameter) results in an effective blood viscosity that is strongly dependent on microvessel diameter and a departure from this relationship.

PRESSURE AND FLOW RELATIONS IN THE MICROVASCULAR NETWORK

Direct measurements of pressures and flows in exteriorized tissues have provided a wealth of data on microvascular hemodynamics throughout successive microvascular divisions (77). Relating these data to the architecture of the microvascular network has presented a challenging problem. The disparate topography of arterioles, capillaries, and venules among numerous tissues (e.g., mesentery, omentum, intestine, striated muscle) has prompted a search for methods to discern commonalities in structure and function among various tissues. As typified in Figure 1 for the mesenteric circulation (cat) (75), the distribution of intravascular pressures (determined by the servo-null method (33; 73)) and red cell velocity (two-slit method (71)) is presented using vessel lumen width (assumed equal to internal diameter) as an index of position within the hierarchy of microvessels. The increasingly precipitous decline in arterial pressure with diminishing diameters reflects a steady rise in resistance to flow for the entire throughput of the network. It is evident that the resistance to flow within each major architectural division (arterioles, precapillaries, capillaries, etc.) attains a maximum in the precapillary vessels; in contrast to the expectation that the maximum resistance (R) occurs in the smallest vessels, based upon Poiseuille's law, where $R = \Delta P/Q = (128/\pi)(\eta l/D^4)$. The steady decline in red cell velocity in the arteriolar network, and its subsequent rise in venular segments, represent conservation of the total throughput of the network as the number of vessels varies through sequential segments. These trends have been shown to be indicative of the unique branching patterns of many tissues, as
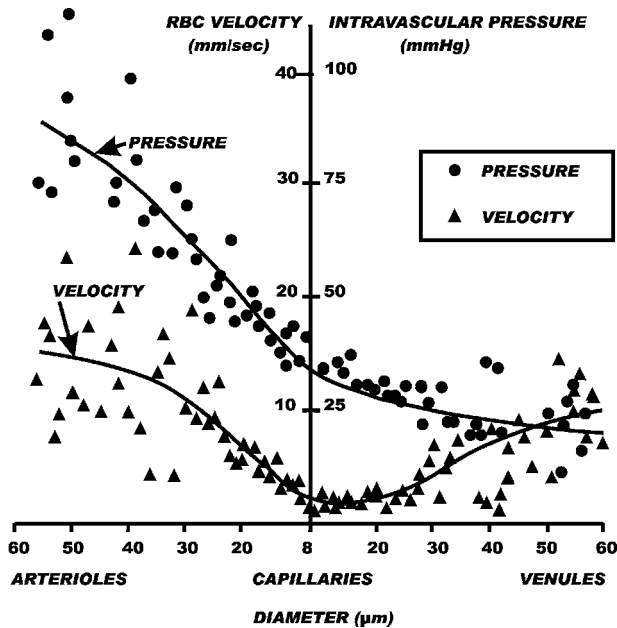
Figure 1. Arteriovenous distribution of intravascular pressure and red cell velocity from arterioles to venules in mesentery (cat) obtained in the laboratory of Benjamin W. Zweifach (75) (with permission). Microvessel diameter (abscissa) is taken as an index of position within the network. Pressure falls in accord with the resistance to flow through successive divisions, which is dependent on network topography and the viscous properties of blood.

described by the late Benjamin W. Zweifach, who in a long and distinguished career pioneered many studies of hemodynamics in the microvasculature, nurtured the development of the methodology to perform such studies, and stimulated and inspired many of his students to continue in his footsteps.

Whereas such spatial distributions of hemodynamic parameters loosely correlate with form and function of the microvascular network, their ability to reveal insights into the relationship between the total throughput of the network and demands of the parenchymal tissue is somewhat limited. Other schemes to relate hemodynamics to function have revolved around centripetal and centrifugal order of branching schemes (72), the application of Strahler's and Horton's laws that describe the topography of river patterns (23), a combination of the two schemes (16), expressing hemodynamics in terms of generations of branching (40), fractal representation of topography and flows (26), or spatial patterns of bundles of microvessels (66). Dynamic studies of the dispersion of indicators throughout the microvascular network (50) have highlighted the difficulty in

delineating the order of perfusion of divisions of a given network. The appearance of indicators (labeled plasma or red cells) within the venular network often precedes that in nearby arterioles, thus suggesting a multiplicity of pathways from inlet to outlet in most networks. It is evident that the microvascular network cannot be simply expressed as an ensemble of purely serial and parallel elements (24). The multiplicity of pathways to the true capillaries may result in a functional capillary density that is flow dependent. It has been shown that flow reductions within an individual capillary may have a minimal effect on arteriolar flow (51). Computer simulations of flow through skeletal muscle reveal an invariance of resistance to flow through the network until greater than 30% of all capillaries are occluded (32).

WALL SHEAR STRESS

Hydrodynamic shear stresses acting on the endothelium are now recognized as important determinants of mechanotransduction and the release of vasoactive substances (6). Recent studies have demonstrated that the coupling of blood rheological properties and vasoregulatory behavior may dramatically affect capillary perfusion. In studies of blood substitutes, it has been shown that an elevated viscosity elicits a vasodilatory response due to increased shear stresses that enhances flow within capillaries (10).

In vitro studies with glass tubes by Barbee and Cokelet (3) paved the way for a realistic appraisal of shear rates and stresses throughout the microvascular tree. Using glass tubes as small as 29 μm, these studies demonstrated that shear stress in tubes of microvessel dimensions could be described in terms of shear rates (regardless of tube size) provided that the tube hematocrit was correctly specified. Thus, given the correct tube hematocrit, the relationship between blood viscosity and shear rates in microvessels could be uniquely specified for tubes representative of arterioles and venules. *In vivo* estimates of effective viscosity from upstream to downstream pressure drop (ΔP) and flow in small arterioles were in general agreement with these studies (46). Whereas the *in vivo* measurement of upstream to downstream pressure drops in single unbranched microvessels is technically challenging, the value of the information may far exceed the inherent errors and uncertainties. Values of wall shear stress (τ_{WALL}) have been obtained by direct measurement of ΔP and vessel length l and diameter D (44). Assuming a vessel of uniform diameter and circular cross section,

application of the principle of static equilibrium dictates that $\tau_{\text{WALL}} = \Delta PD/4l$. Thus, with these assumptions, τ_{WALL} was found to average 47 dyn/cm^2 in arterioles and 29 dyn/cm^2 in venules of the mesentery (cat) in the normal flow state (44).

The foundation laid down by *in vitro* rheological studies facilitated estimation of shear rates and stresses throughout the microvasculature based on direct measurements of red cell velocity and microvessel geometry in tissues such as mesentery (76), cremaster muscle (31), and spinotrapezius muscle (77), as illustrated in Figure 2. These distributions of shear rates $\dot\gamma$ were calculated from measurements of red cell velocity (V_{RBC}, two-slit method) using empirical correlations between volumetric flow and V_{RBC} obtained in glass tubes (2). Using an effective value of blood viscosity obtained in mesentery, shear stresses τ_{WALL} were estimated from the Newtonian relationship $\tau_{\text{WALL}} = \eta\dot\gamma$, assuming a value of $\eta = 3.5$ cP (44). These data reveal shear stresses in arterioles ranging from 25–60 dyn/cm^2, which fall dramatically to 10–30 dyn/cm^2 in postcapillary venules, in the normal flow state (43).

RESISTANCE

The resistance R to flow arises from the effective viscosity η of blood and vascular hindrance z, such that $R = \eta z$. Using Poiseuille's law as a model, the resistance per unit length (R/L) of microvessel at a given η should be inversely proportional to D^4. Direct measurements of upstream to downstream pressure drop in single unbranched microvessels using the dual servo-null technique (46) and flow (two-

slit technique (2,47,71)) permitted calculation of R/L (from $R = \Delta P/Q$ and vessel length) to reveal a four-decade increase in R/L (44) as blood traverses the arteriolar network in mesentery (cat). Remarkably, a power law regression against D revealed an exponent of 4.0 on the arteriolar side and 3.9 on the venous side of the capillary network. Thus, in the normal flow state, the fourth-power dependency on diameter is the dominant determinant of resistance to flow. Although the conditions for which Poiseuille's law applies (uniform fluid with constant viscosity) are not readily applicable to the microcirculation, the broad range of diameters encountered as blood traverses the network from arteriole to capillary results in a dominance of the fourth power of diameter. This behavior is of great importance since small changes in vascular diameter may result in a fourfold greater change in resistance within individual microvessels, thus affecting the distribution of flow within the microvascular network.

APPARENT VISCOSITY

Using Poiseuille's law as a constitutive equation for blood flow in microvessels, the apparent viscosity η of blood may be computed from measured pressure drops and flows. The measurement of upstream to downstream pressure drops poses many challenges. Cumulative errors in the calculation of η may amount to 46% (46). The major determinants of *in vivo* apparent viscosity are shear rates and tube hematocrit. At the low level of microvascular hematocrits found in most tissues in the normal flow state, the apparent viscosity varies linearly with microvessel hematocrit (H_{MICRO}) (45). These studies have revealed average arteriolar values of about 3.6 cP and average venular values of about 5.2 cP in the mesentery of the cat. The greater viscosity in venules was attributed to the relatively lower shear rates, leukocyte adhesion to the walls of venules that may obstruct the lumen and give a falsely elevated viscosity, and greater departures from a circular cross section. As flow rates are decreased, such as in shock, hemorrhage, and other circulatory disorders, flow within individual microvessels falls nonlinearly with pressure drop, suggesting increases in the apparent viscosity of blood (44). Determination of the variation of effective viscosity with shear rate and diameter by indirect analysis, using computations of pressures and flows throughout the mesentery (rat) to match measured red cell fluxes and boundary pressures, have resulted in a self-consistent appraisal of effective viscosity that falls between *in vitro* tube studies and direct *in situ* measurements
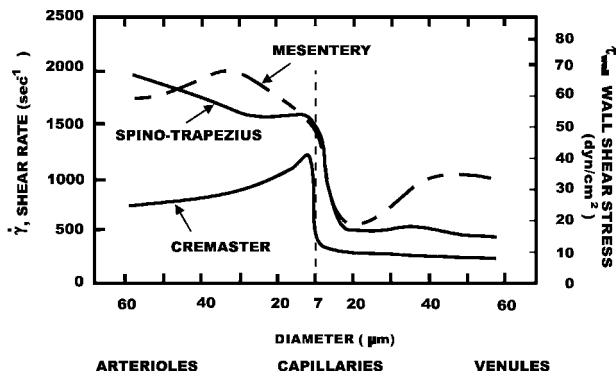
Figure 2. Arteriovenous distribution of wall shear rate ($\dot\gamma$, based on measured V_{RBC} and diameter), and wall shear stress, τ_{WALL}, calculated from the product of $\dot\gamma\eta$ assuming that $\eta = 3.5$ cP for 3 representative microvascular networks (from (43), with permission).

(57), although considerable errors may be present due to inaccuracies in accounting for the true geometry of the vessel cross section in the measurements (14).

MICROVASCULAR HEMATOCRIT

The pioneering studies of Fåhraeus (20) on blood flow in small-bore glass tubes revealed that two hematocrits are necessary to describe blood within the microcirculation: The tube, or microvessel hematocrit (H_{MICRO}), represents the red cell fraction resident in the tube at any instant of time, and the discharge hematocrit (H_{DISCH}) is the red cell fraction of the effluent of a tube, collected in a hypothetical mixing cup. The disparity between tube and discharge hematocrit arises with reductions in tube diameter because the mean velocity of red cells increases relative to mean plasma velocity, hence fewer cells must be resident within the tube to ensure that the discharge hematocrit equals the feed hematocrit. Tube hematocrit falls as diameter is decreased until a minimum diameter is reached, below which deformation of RBCs lead to their sequestration (1). Poiseuille (67) observed the skimming of plasma from side branches in small blood vessels. These two processes lead to a decrease in microvessel hematocrit as blood courses its way from arterioles to capillaries and a subsequent rise in postcapillary venules. Studies by Barbee and Cokelet (4) and others on the effect of tube diameter and Fenton, Carr, and Cokelet (22) on plasma skimming at bifurcations have provided a basis for understanding *in vivo* observations. *In vivo* measurements of H_{MICRO} in networks such as the cheek pouch (61), cremaster muscle (36) and mesentery (45) have suggested that these effects are dependent on network topography and local flow rates. It is thought that the heterogeneity in red cell velocity and microvessel hematocrit within any given microvascular division may contribute to about 20% of the total reduction in capillary hematocrit (55).

It has been suggested that H_{MICRO} is relatively uniform across the lumen (radial direction) of an arteriole or venule, compared with the heterogeneity associated with successive branchings. However, the presence of a thin annulus of plasma surrounding the core of RBCs within a microvessel facilitates an uneven distribution of RBCs at arteriolar branchings (12). The proportion of RBCs from the core and cell-free plasma layer that is captured by an arteriolar branch at a bifurcation is dependent upon the relative magnitudes of total volumetric flow from par-

ent to daughter branch at a bifurcation. At the final ramifications of the arteriolar network, red cell entry into capillaries is dependent on the presence of a sufficient pressure gradient that can sustain red cell deformations at the capillary entrance, hence the capillary branch with the fastest stream (greatest pressure gradient) captures the majority of red cells. If one averages daughter to parent branch ratios of red cell flux and their respective bulk flow ratios over many bifurcations, these effects appear to be greatly attenuated and RBC flux and bulk flow rates follow 1:1 within a small deviation (37). However, for an individual bifurcation, the relationships between cell flux and flow are strongly nonlinear (sigmoidal) (62). The forces that govern phase separation (cells from plasma) of blood have been described in terms of the hydrodynamic forces (25,62,74). Radial forces arise from the summated effects of shear stress and the pressure distribution on individual cells that direct cells into the daughter branch with the greater flow rate. Similar dynamics have been revealed for the case of WBCs negotiating bifurcations in the network (41).

Low values of H_{MICRO} relative to systemic hematocrit (H_{SYS}) suggest that oxygen transport to tissue may be compromised by diminished oxygen-carrying capacity. Direct intubation of microvessels with micropipettes to aspirate the red cell flux has suggested that the discharge hematocrit (H_{DISCH}) agrees well with H_{SYS} (17) for microvessels ranging in diameter from 6 to 98 μm. Calculations of an average tissue hematocrit, based upon the relative transit times of plasma and red cells measured within the microvascular network have revealed a close agreement with H_{SYS} (52).

BLOOD CELL DEFORMABILITY

With diminishing vessel diameter, the particulate nature of blood dominates the resistance to flow. *In vitro* simulation of capillary flows using polycarbonate sieves with 5 μm pores (Nuclepore filters) was pioneered by Gregersen et al. (27) and emphasized the dominant contribution of red cell deformability to perfusion of capillaries. Through such experimental simulations it is now recognized that the initial deformation that red blood cells (RBCs) and white blood cells (WBCs) incur upon entry to a capillary contributes significantly to the pressure drop across individual capillaries (42,62,64). Thus, the contribution of the intrinsic properties of blood to hemodynamic resistance changes markedly throughout the

succession of vessels from arterioles to capillaries as diameter varies between divisions.

Blood cell deformability affects the entrance of blood cells into capillaries. RBCs with reduced deformability in pathological disorders (e.g., sickle cell disease) may be sequestered at the capillary entrance. Stiffening of the red cell membrane or elevations in hemoglobin viscosity may impede RBC transit through capillaries (28,34,52). The normally stiffer WBCs traverse the capillary network through larger thoroughfare channels (19) and WBCs may become trapped at the capillary entrance or incur a prolonged transit time following their stiffening with activation during inflammation (5, 29).

BLOOD CELL AGGREGATION

The effect of red cell aggregation (RCA) on the *in vivo* resistance to flow has been fraught with controversy. *In vitro* studies of RCA in vertically positioned, small-bore glass tubes (13,59,60) revealed that apparent viscosity decreases with increasing degrees of RCA. However, *in vivo* measurements in the low flow state suggest a dramatic rise in apparent viscosity with reductions in $\dot{\gamma}$ based on resistance measurements within individual venules (44) or isolated regions of skeletal muscle (9). Studies of aggregate formation in postcapillary venules in response to high molecular weight dextrans (500 kDa) reveal a blunting of the velocity profile that may result in greater energy dissipation and hence increased resistance (7). Studies of the radial dispersion of RBCs during dextran-induced aggregation suggest that the succession of branches in the venous circulation attenuates axial migration of RBCs (8), thus inhibiting the development of an annular plasma layer as occurs in the relatively longer unbranched tubes *in vitro*.

It is apparent that the effects of RCA vary between regional networks as well as within a discrete ensemble of microvessels perfused by the same source. To illustrate, shown in Figure 3 is the variation of resistance between a paired arteriole and venule that serve the single inflow/outflow modular network of microvessels peculiar to the rabbit omentum. Arteriovenous resistance (R_{AV}) was computed from the ratio of arteriolar–venular pressure drop (dual servo-null method, (46)) to the volumetric flow measured in the feeding arteriole (two-slit method, (47)). With infusion of successively greater levels of high molecular weight dextran (500 kDa; D × 500) R_{AV} first rises slightly, as plasma viscosity increases, and then falls precipitously as [D × 500] exceeds 1 g%. These
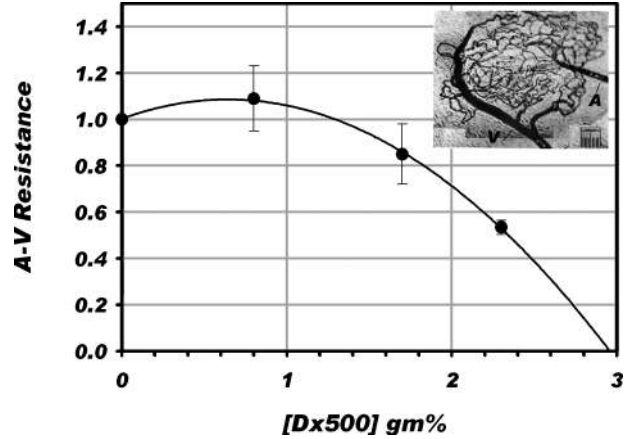
Figure 3. Arteriole to venule resistance obtained in a single inlet/outlet module of the rabbit omentum (inset) for various plasma concentrations of high molecular weight dextran (500 kDa, D × 500). The resistance was computed from $R = \Delta P/Q$, where Q was obtained from V_{RBC} in the feeding arteriole. With increasing [D × 500] R initially rises as plasma viscosity becomes elevated and then falls dramatically as red cell aggregation causes a marked reduction in systemic hematocrit as RBCs are sequestered in other organs. Arteriolar microvessel hematocrit fell from 26 to 13% as H_{SYS} fell from 33 to 20% as [D × 500] rose to 2.6 g%. These trends suggest that the response to extreme red cell aggregation may be quite variable among different networks, with some showing severe increases in red cell entrapment, and others showing severe hemodilution.

trends arise because of red cell sequestration in other organs with increasing RCA that leads to a dramatic decrease in H_{SYS} and H_{MICRO} in the arteriole. In this particular case, arteriolar H_{MICRO} fell from 25.6 to 13.1% as H_{SYS} fell from 32.5 to 20.0% in response to [D × 500] increasing from 0 to 2.6 g%.

In vitro and theoretical studies have provided a biophysical foundation for understanding the relationship between shearing forces and the strength of red cell aggregation. Skalak et al. (65) have shown that as strength of aggregation increases, RBCs form rouleaux and then clumps. With greater degrees of cross-bridging by macromolecules to form aggregates, apposing red cell membranes bind more tightly and aggregates undergo a transition from rouleaux to clumps, as illustrated in Figure 4A, B. *In vivo* studies have demonstrated that rouleaux are much more easily disrupted at bifurcations, whereas clumps may become lodged at the entrance to capillaries (53), as illustrated in Figure 4C, where rouleaux, induced by 0.7 g% fibrinogen, pile up at a bifurcation in the low-flow state. Increasing the strength of aggregation with 3 g% D × 500 resulted in clumps of
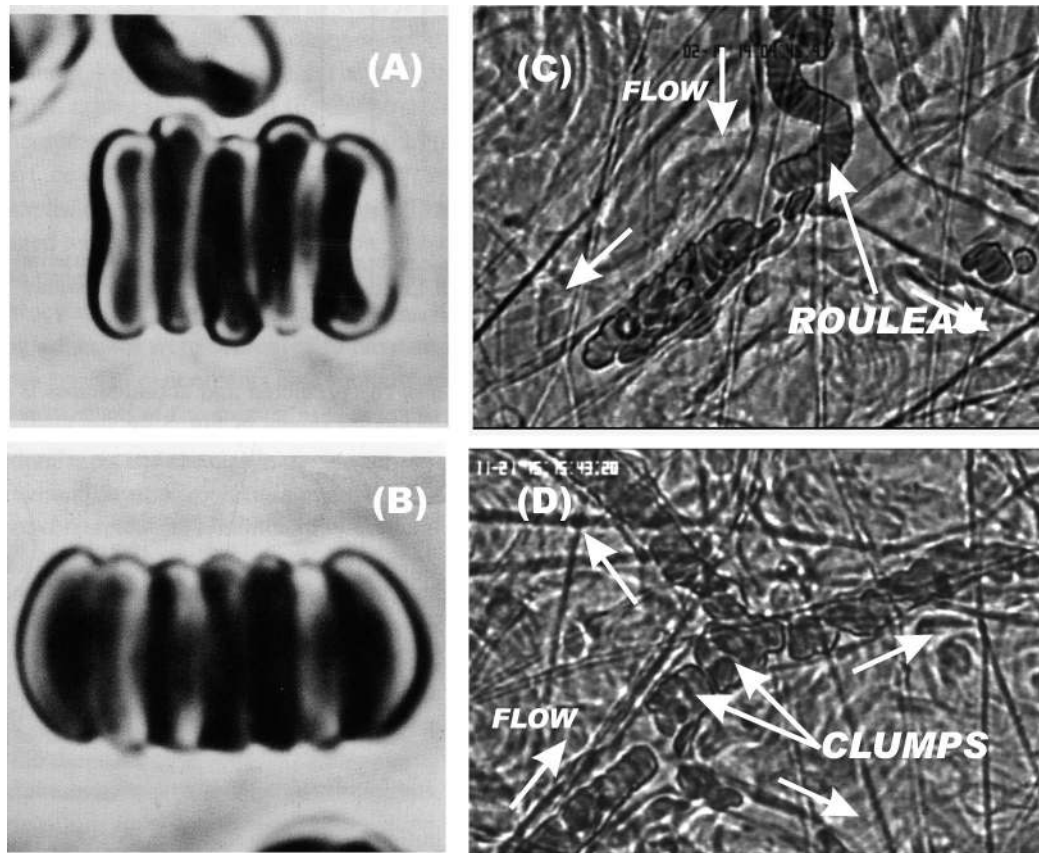
Figure 4. As the strength of red cell aggregation increases, aggregates undergo a transition from rouleaux (A) to clumps (B) (from (65), with permission). The weaker rouleaux that tend to pile up at branch points in the arteriolar network (C) in the low flow state are easily disrupted compared to the stronger clumps (D) that become lodged at the entrance to capillaries and resist disruption upon recovery from a low flow state (from (53), with permission).

RBCs that frequently became lodged at the capillary entrance and resisted disruption by hydrodynamic forces.

BLOOD CELL–ENDOTHELIUM INTERACTIONS

The adhesive interactions of RBCs and WBCs with the endothelium in, for example, sickle cell disease and inflammation, respectively, have prompted rheological studies of the effect of blood cell adhesion on flow resistance, the molecular basis for adhesion and the effect of hydrodynamic forces on the dynamics of adhesion. In experimental models of inflammation, it has been shown that as few as 12 WBCs adhering per 100 μm of venule length may double the resistance to flow in postcapillary venules (30). Significant retardation of flow may occur when sickle red cells adhere to the microvessel wall and obstruct the lumen (34). These events may initiate a further decline in flow

leading to the sequence of red cell deoxygenation, hemoglobin polymerization and further cell sequestration (35).

It has been demonstrated that the endothelial cell glycocalyx may influence both red cell flux through capillaries, as well as leukocyte contact with the endothelium. By perfusing capillaries with heparinase to enzymatically degrade heparam sulfate glycosaminoglycans (GAGs) on the endothelial cell surface, Desjardins and Duling (18) have shown that capillary hematocrit may increase almost threefold due to an increase in the effective lumen diameter. Subsequent studies by Vink and Duling (69, 70) demonstrated that red cells and macromolecules have a limited access to the endothelial membrane. As illustrated in Figure 5A under bright field microscopy and Figure 5B under fluorescence microscopy, RBCs, and FITC-dextran reveal a capillary width that is 0.8–1 μm less than the anatomical width, thus suggesting
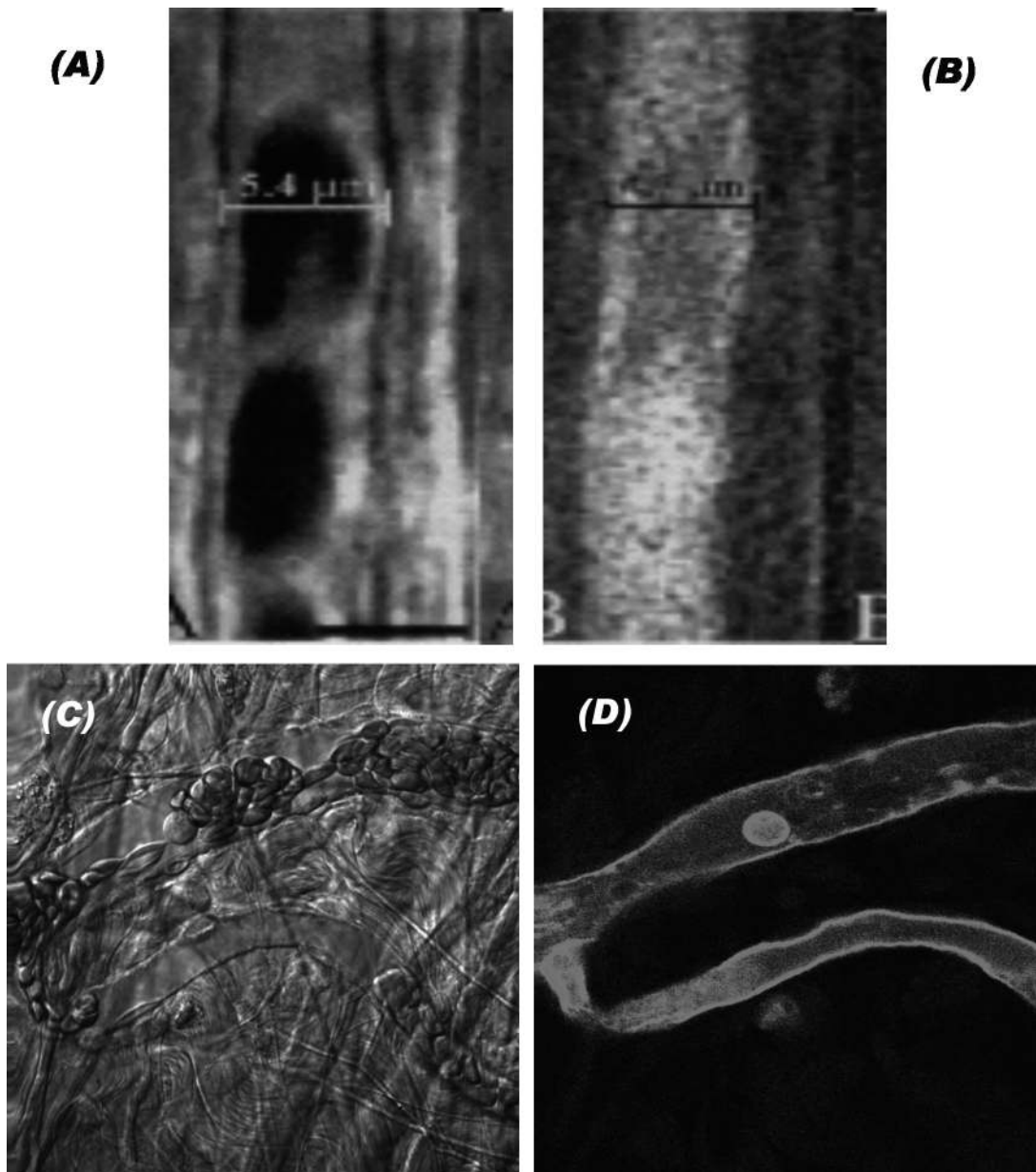
Figure 5. Vink and Duling have demonstrated that red cells and macromolecules have limited access to the endothelial cell membrane due to the presence of a 0.4 to 0.5-mm-thick endothelial surface layer. As shown above under bright field (A) and fluorescence (B) microscopy, the width of either a red cell column (A) or fluorescent dextran (B) is significantly less than the anatomical width of the capillary lumen (from (69) with permission). Direct staining of sugars in the glycocalyx with fluorescent lectins (D) reveals the presence of this surface layer within the lumen of postcapillary venules, shown in (C) under brightfield microscopy. Shedding of components of the glycocalyx have been observed in response to the chemoattractant fMLP and ischemia (from (49), with permission). This event may increase accessibility of adhesion molecules (ICAM-1) to WBCs (48).

the presence of an endothelial surface layer 0.4–0.5 μm in thickness (69). These studies are consistent with the presence of a thick endothelial layer comprising a broad range of proteoglycans and GAGs, that has been observed to extend from 0.5 to over 1 μm in fixed endothelium (56). Computer simulations of capillary blood flow suggest that the presence of a thick endothelial surface layer in capillaries may

significantly affect red cell flux, and that its deformation with fluid shear stresses may enhance the ability of red cells to traverse nonuniform capillaries (63).

Enzymatic degradation of the glycocalyx by infusion of heparinase in mesenteric arterioles has resulted in a decrease in regional resistance up to 21% (58). It has been demonstrated that removal of heparan sulfate GAGs by perfusion of mesenteric post-capillary venules with heparinase results in increased WBC-EC adhesion (48). Similar findings have been noted in cremaster muscle in response to infusion of oxidized LDL (15). Superfusion of mesenteric tissue with the peptide fMLP (f-met-leu-phe) results in a rapid increase in the adhesion of inert microspheres labeled with antibody for ICAM-1(48), thus suggesting that elements of the endothelial surface layer were being shed to result in greater exposure of ICAM-1 that was buried in the glycocalyx. In support of this hypothesis, studies were conducted to quantify the adhesion of fluorescent microspheres coated with lectins or FITC-conjugated lectins, specific for glucosaminoglycans or galactosaminoglycans (49). Illustrated in Figure 5C (bright-field) and 5D (fluorescence) is the accumulation of FITC labeled lectin specific for galactosaminoglycans (49). These studies revealed a time-dependent reduction in lectin label following superfusion with fMLP. A similar reduction was observed during reperfusion following a 60-min period of normoxic ischemia. These responses were suggestive of glycan shedding and could be inhibited by G-protein inhibition with pertussis toxin. Hence it appears that the thickness of the endothelial surface layer may reflect, at any time, a balance of continued biosynthesis of glycans and their shear-dependent removal.

CONCLUSIONS

Rheological studies of blood flow in the microcirculation by members of the Microcirculatory Society have provided a wealth of information on factors that affect control and regulation of the terminal vascular network and the delivery of oxygen to tissue. Some of these observations include (1) the overwhelming dominance of D^4 as a determinant of resistance to flow within individual microvessels, (2) that microvessel hematocrit is a principal determinant of effective viscosity and oxygen transport to tissue and is strongly dependent on network topography, (3) that mechanical properties of RBCs and WBCs may influence perfusion and the convective transport of oxygen to tissue, (4) that adhesive interactions between blood cells and the endothelium are important determinants of the resistance to flow and recovery from an ischemic flow state, and (5) that the molecular interactions of blood cells with one another (red cell aggregation) and with the endothelial glycocalyx may govern the function of inflammatory cells and reperfusion following ischemia. It should be readily apparent that studies of the rheological behavior of blood flow within the microvasculature necessitate an understanding of the interaction between flow distribution throughout the network and blood viscous behavior within individual microvessels. This goal appears to be a challenging task, but one with potentially great benefits toward unraveling the mysteries of the microcirculation.

REFERENCES

1. Albrecht KH, Gaehtgens P, Pries A, Heuser M. (1979). The Fahraeus effect in narrow capillaries (i.d. 3.3 to 11.0 micron). *Microvasc Res* 18:33–47.
2. Baker M, Wayland H. (1974). On-line volume flow rate and velocity profile measurement for blood in microvessels. *Microvasc Res* 7:131–143.
3. Barbee JH, Cokelet GR. (1971). Prediction of blood flow in tubes with diameters as small as 29 microns. *Microvasc Res* 3:17–21.
4. Barbee JH, Cokelet GR. (1971). The Fahraeus effect. *Microvasc Res* 3:6–16.
5. Bathe M, Shirai A, Doerschuk CM, Kamm RD. (2002). Neutrophil transit times through pulmonary capillaries: the effects of capillary geometry and fMLP-stimulation. *Biophys J* 83:1917–1933.
6. Bevan JA, Kaley G, Rubanyi GM. (1995). *Flow-Dependent Regulation of Vascular Function*. New York: Oxford University Press.
7. Bishop JJ, Nance PR, Popel AS, Intaglietta M, Johnson PC. (2001) Effect of erythrocyte aggregation on velocity profiles in venules. *Am J Physiol Heart Circ Physiol* 280:H222–H236.
8. Bishop JJ, Popel AS, Intaglietta M, Johnson PC. (2001). Effects of erythrocyte aggregation and venous network geometry on red blood cell axial migration. *Am J Physiol Heart Circ Physiol* 281:H939–H950.
9. Cabel M, Meiselman HJ, Popel AS, Johnson PC. (1997). Contribution of red blood cell aggregation to venous vascular resistance in skeletal muscle. *Am J Physiol* 272:H1020–H1032.
10. Cabrales P, Tsai AG, Intaglietta M. (2004). Microvascular pressure and functional capillary density in extreme hemodilution with low- and high-viscosity dextran and a low-viscosity Hb-based O_2 carrier. *Am J Physiol Heart Circ Physiol* 287:H363–H373.
11. Chien S, Usami S, Dellenback J, Magazinovic V. (1972) Blood rheology after hemorrhage and endotoxin. *Adv Exp Med Biol* 33:75–93.

12. Cokelet GR. (1999) Poiseuille Award Lecture: viscometric, in vitro and in vivo blood viscosity relationships: how are they related? *Biorheology* 36:343–358.

13. Cokelet GR, Goldsmith HL. (1991) Decreased hydrodynamic resistance in the two-phase flow of blood through small vertical tubes at low flow rates. *Circ Res* 68:1–17.

14. Cokelet GR, Pries AR, Kiani MF. (1998). Observations on the accuracy of photometric techniques used to measure some in vivo microvascular blood flow parameters. *Microcirculation* 5:61–70.

15. Constantinescu AA, Vink H, Spaan JA. (2003). Endothelial cell glycocalyx modulates immobilization of leukocytes at the endothelial surface. *Arterioscler Thromb Vasc Biol* 23:1541–1547.

16. Davis MJ, Ferrer PN, Gore RW. (1986). Vascular anatomy and hydrostatic pressure profile in the hamster cheek pouch. *Am J Physiol* 250:H291–H303.

17. Desjardins C, Duling BR. (1987). Microvessel hematocrit: measurement and implications for capillary oxygen transport. *Am J Physiol* 252:H494–H503.

18. Desjardins C, Duling BR. (1990). Heparinase treatment suggests a role for the endothelial cell glycocalyx in regulation of capillary hematocrit. *Am J Physiol* 258:H647–H654.

19. Eppihimer MJ, Lipowsky HH. (1994). Leukocyte sequestration in the microvasculature in normal and low flow states. *Am J Physiol* 267:H1122–H1134.

20. Fahraeus R. (1929). The suspension stability of blood. *Physiol Rev* 9:241–274.

21. Fåhraeus R, Lindqvist T. (1931). The viscosity of the blood in narrow capillary tubes. *Am J Physiol* 96:562–568.

22. Fenton BM, Carr RT, Cokelet GR. (1985). Nonuniform red cell distribution in 20 to 100 micrometers bifurcations. *Microvasc Res* 29:103–126.

23. Fenton BM, Zweifach BW. (1981). Microcirculatory model relating geometrical variation to changes in pressure and flow rate. *Ann Biomed Eng* 9:303–331.

24. Frasher WG Jr, Wayland H. (1972). A repeating modular organization of the microcirculation of cat mesentery. *Microvasc Res* 4:62–76.

25. Fung YC. (1973). Stochastic flow in capillary blood vessels. *Microvasc Res* 5:34–48.

26. Glenny RW, Robertson HT, Yamashiro S, Bassingthwaighte JB. (1991). Applications of fractal analysis to physiology. *J Appl Physiol* 70:2351–2367.

27. Gregersen MI, Bryant CA, Hammerle WE, Usami S, Chien S. (1967). Flow characteristics of human erythrocytes through polycarbonate sieves. *Science* 157:825–827.

28. Hakim TS. (1994). Effect of erythrocyte heat treatment on pulmonary vascular resistance. *Microvasc Res* 48:13–25.

29. Harris AG, Skalak TC. (1996). Effects of leukocyte capillary plugging in skeletal muscle ischemia–reperfusion injury. *Am J Physiol* 271:H2653–H2660.

30. House SD, Lipowsky HH. (1987) Leukocyte-endothelium adhesion: microhemodynamics in mesentery of the cat. *Microvasc Res* 34:363–379.

31. House SD, Lipowsky HH. (1987). Microvascular hematocrit and red cell flux in rat cremaster muscle. *Am J Physiol* 252:H211–H222.

32. Hudetz AG. (1993). Percolation phenomenon: the effect of capillary network rarefaction. *Microvasc Res* 45:1–10.

33. Intaglietta M, Pawula RF, Tompkins WR. (1970). Pressure measurements in the mammalian microvasculature. *Microvasc Res* 2:212–220.

34. Kaul DK, Fabry ME. (2004). In vivo studies of sickle red blood cells. *Microcirculation* 11:153–165.

35. Kaul DK, Fabry ME, Costantini F, Rubin EM, Nagel RL. (1995). In vivo demonstration of red cell–endothelial interaction, sickling and altered microvascular response to oxygen in the sickle transgenic mouse. *J Clin Invest* 96:2845–2853.

36. Klitzman B, Duling BR. (1979). Microvascular hematocrit and red cell flow in resting and contracting striated muscle. *Am J Physiol* 237:H481–H490.

37. Klitzman B, Johnson PC. (1982). Capillary network geometry and red cell distribution in hamster cremaster muscle. *Am J Physiol* 242:H211–H219.

38. Krogh A. (1922). *The Anatomy and Physiology of the Capillaries*. New Haven, CT: Yale University Press.

39. Landis EM. (1933). Poiseuille's law and the capillary circulation. *Am J Physiol* 103:432–443.

40. Ley K, Pries AR, Gaehtgens P. (1986). Topological structure of rat mesenteric microvessel networks. *Microvasc Res* 32:315–332.

41. Ley K, Pries AR, Gaehtgens P. (1988). Preferential distribution of leukocytes in rat mesentery microvessel networks. *Pflugers Arch* 412:93–100.

42. Lingard PS. (1974). Capillary pore rheology of erythrocytes, 1: hydroelastic behaviour of human erythrocytes. *Microvasc Res* 8:53–63.

43. Lipowsky HH. (1995). Shear stress in the circulation. In: *Flow-Dependent Regualation of Vascular Function* (JA Bevan, G Kaley, GM Rubanyi, Eds.) New York, NY: Oxford University Press.

44. Lipowsky HH, Kovalcheck S, Zweifach BW. (1978). The distribution of blood rheological parameters in the microvasculature of cat mesentery. *Circ Res* 43:738–749.

45. Lipowsky HH, Usami S, Chien S. (1980). In vivo measurements of "apparent viscosity" and microvessel hematocrit in the mesentery of the cat. *Microvasc Res* 19:297–319.

46. Lipowsky HH, Zweifach BW. (1977). Methods for the simultaneous measurement of pressure differentials and flow in single unbranched vessels of the microcirculation for rheological studies. *Microvasc Res* 14:345–361.

47. Lipowsky HH, Zweifach BW. (1978). Application of the "two-slit" photometric technique to the

measurement of microvascular volumetric flow rates. *Microvasc Res* 15:93–101.

48. Mulivor AW, Lipowsky HH. (2002). Role of glycocalyx in leukocyte–endothelial cell adhesion. *Am J Physiol Heart Circ Physiol* 283:H1282–H1291.

49. Mulivor AW, Lipowsky HH. (2004). Inflammation- and ischemia-induced shedding of venular glycocalyx. *Am J Physiol Heart Circ Physiol* 286:H1672–H1680.

50. Nellis SH, Lee JS. (1974). Dispersion of indicator measured from microvessels of cat mesentery. *Circ Res* 35:580–591.

51. Nellis SH, Zweifach BW. (1977). A method for determining segmental resistances in the microcirculation from pressure–flow measurements. *Circ Res* 40:546–556.

52. Parthasarathi K, Lipowsky HH. (1999). Capillary recruitment in response to tissue hypoxia and its dependence on red blood cell deformability. *Am J Physiol* 277:H2145–H2157.

53. Pearson MJ, Lipowsky HH. (2004). Effect of fibrinogen on leukocyte margination and adhesion in postcapillary venules. *Microcirculation* 11:295–306.

54. Poiseuille JLM. (1840). Rechershes expérimentales sur le mouvement des liquides dans les tubes de très petits diamètres. *CR Acad Sci* 11:961–967.

55. Pries AR, Ley K, Gaehtgens P. (1986). Generalization of the Fahraeus principle for microvessel networks. *Am J Physiol* 251:H1324–H1332.

56. Pries AR, Secomb TW, Gaehtgens P. (2000). The endothelial surface layer. *Pflugers Arch* 440: 653–666.

57. Pries AR, Secomb TW, Gessner T, Sperandio MB, Gross JF, Gaehtgens P. (1994). Resistance to blood flow in microvessels in vivo. *Circ Res* 75:904–915.

58. Pries AR, Secomb TW, Jacobs H, Sperandio M, Osterloh K, Gaehtgens P. (1997). Microvascular blood flow resistance: role of endothelial surface layer. *Am J Physiol* 273:H2272–H2279.

59. Reinke W, Gaehtgens P, Johnson PC. (1987). Blood viscosity in small tubes: effect of shear rate, aggregation, and sedimentation. *Am J Physiol* 253:H540–H547.

60. Reinke W, Johnson PC, Gaehtgens P. (1986). Effect of shear rate variation on apparent viscosity of human blood in tubes of 29 to 94 microns diameter. *Circ Res* 59:124–132.

61. Sarelius IH, Duling BR. (1982). Direct measurement of microvessel hematocrit, red cell flux, velocity, and transit time. *Am J Physiol* 243:H1018–H1026.

62. Schmid-Schonbein GW, Skalak R, Usami S, Chien S. (1980). Cell distribution in capillary networks. *Microvasc Res* 19:18–44.

63. Secomb TW, Hsu R, Pries AR. (2002). Blood flow and red blood cell deformation in nonuniform capillaries: effects of the endothelial surface layer. *Microcirculation* 9:189–196.

64. Skalak R, Soslowsky L, Schmalzer E, Impelluso T, Chien S. (1987). Theory of filtration of mixed blood suspensions. *Biorheology* 24:35–52.

65. Skalak R, Zarda PR, Jan KM, Chien S. (1981). Mechanics of Rouleau formation. *Biophys J* 35:771–781.

66. Skalak TC, Schmid-Schonbein GW. (1986). The microvasculature in skeletal muscle, IV: a model of the capillary network. *Microvasc Res* 32:333–347.

67. Sutera SP, Skalak R. (1993). The history of Poiseuille's law. *Annu Rev Fluid Mech* 25:1–20.

68. Vejlens G. (1938). The distribution of leukocytes in the vascular system. *Acta Pathol Microbiol Scand Suppl* 33:3–239.

69. Vink H, Duling BR. (1996). Identification of distinct luminal domains for macromolecules, erythrocytes, and leukocytes within mammalian capillaries. *Circ Res* 79:581–589.

70. Vink H, Duling BR. (2000). Capillary endothelial surface layer selectively reduces plasma solute distribution volume. *Am J Physiol Heart Circ Physiol* 278:H285–H289.

71. Wayland H, Johnson PC. (1967). Erythrocyte velocity measurement in microvessels by a correlation method. *Bibl Anat* 9:160–163.

72. Wiedeman MP. (1984). Architecture. In: *Handbook of Physiology*, Section 2: *The Cardiovascular System*, Vol IV: *Microcirculation* (EM Renkin, CC Michel, Eds.) Bethesd, MD: American Physiological Society, 11–40.

73. Wiederhielm CA, Woodbury JW, Kirk S, Rushmer RF. (1964). Pulsatile pressures in the microcirculation of frog's mesentery. *Am J Physiol* 207:173–176.

74. Yen RT, Fung YC. (1978). Effect of velocity of distribution on red cell distribution in capillary blood vessels. *JR Coll Gen Pract Occas Pap* 235:H251–H257.

75. Zweifach BW. (1974). Quantitative studies of microcirculatory structure and function, I: analysis of pressure distribution in the terminal vascular bed in cat mesentery. *Circ Res* 34:843–857.

76. Zweifach BW, Lipowsky HH. (1977). Quantitative studies of microcirculatory structure and function, III: microvascular hemodynamics of cat mesentery and rabbit omentum. *Circ Res* 41:380–390.

77. Zweifach BW, Lipowsky HH. (1984). Pressure–flow relations in blood and lymph microcirculation. In: *Handbook of Physiology—The Cardiovascular System IV* (EM Renkin, CC Michel, Eds.) Bethesda, MD: American Physiological Society, 251–307.